Supplemental Methods

Cell culture, purification and radiolabeling of anti-EGFR mAb

The MDA-MB-231 cell line (ATCC™, VA, USA), a basal-like TNBC and mesenchymal stem-like cell line, was cultured as per ATCC™ instructions. MDA-MB-231 cells expressing Luciferase were prepared as described here. The hybridoma producing the anti-human EGFR mouse mAb (clone 225 HB-8508, IgG1; ATCC™) was cultured as per ATCC™ instructions. This mouse mAb is the precursor to the derived chimeric human:murine antibody C225, commercially known as cetuximab. All the cell lines were regularly tested for mycoplasma and authenticated using STR profiling.

The mAb was purified, conjugated to 1,4,7,10-tetraazacyclododecane-1,4,7,10-tetraacetic acid N-hydroxysuccinimide ester (DOTA-NHS-ESTER, Macrocyclics, TX, USA) and radiolabeled with ^{177}Lu using $^{177}LuCl_3$ (Perkin Elmer, MA, USA) as described elsewhere (*1*). The specific activity of ^{177}Lu-anti-EGFR mAb ranged between 2 and 3 μCi/μg (74–111 MBq/mg). The radiolabeling efficiency was > 98% as judged by standard ITLC-SG (*10*). ^{177}Lu-anti-EGFR mAb retained > 95% of its immunoreactivity as judged by radioimmunoblotting (autoradiography) against MDA-MB-231 cell lysates in comparison to unlabeled EGFR mAb (data not shown). The stability of ^{177}Lu-anti-EGFR mAb was tested in 10% fetal calf serum in PBS containing 10 μM of EDTA and incubated at 37°C. More than 90% of ^{177}Lu remained attached to the anti-EGFR mAb for at least 48 hours as judged by ITLC and less than 5% degradation was observed in autoradiography of SDS-PAGE fractionation after this incubation.

Luciferase transduction

MDA-MB-231 cells expressing Luciferase were prepared by transduction with the Luciferase expressing retrovirus packaged using the Phoenix amphotrophic cell line and pFB-neo/Luciferase construct (gift from Cameron N. Johnstone, Peter MacCallum Cancer Centre, Melbourne, Australia). Transduced cells were selected for 5 days with 400 μg/mL of G418 (Sigma-Aldrich®, MO, USA).

Mouse models

For the orthotopic models, female BALB/c nude mice at 5 weeks of age (Animal Resources Centre, ARC, WA, Australia) were inoculated in the 4th inguinal mammary fat pad. Exponentially growing Luciferase-expressing MDA-MB-231 cells (5×10^6 per mouse) were injected in 50 μL of 50% PBS and 50% Matrigel™ (Becton Dickinson) solution. The TNBC tumor graft derived from patient HCI-002 (*2*), which stained positive for EGFR (data not shown), was used in our studies. Pieces (~4 mm^3) prepared from *in vivo* passage of HCI-002 were implanted along with 20 μL of Matrigel™ mammary fat pads. For the experimental metastasis model, female BALB/c nude mice at 5 weeks of age were injected by tail vein with 0.5×10^6 Luciferase-expressing MDA-MB-231 cells in PBS per mouse. Metastases were established 14 days after inoculation as determined by Bioluminescence live imaging (BLI). BLI was carried out using IVIS100 live animal imaging system (Caliper Life Sciences, MA, USA) at 10 min after intraperitoneal injection of 125 mg/kg VivoGlow™ Luciferin (Promega Corporation).

EGFR gene expression analysis in published datasets from breast cancer patients

The raw CEL data files from publicly available gene expression array studies (using Affymetrix platforms) were analyzed by RMA method then quantile normalized using BRB-ArrayTools (*3*) (V4.2, Biometric Research Branch, NCI, Maryland, USA). The molecular subtypes of tumors in the datasets were classified using the single sample predictor method developed previously (*4*). Each sample was assigned to a subtype based on the highest Spearman rank correlation to the 306 gene centroids. The expression of EGFR mRNA (log2 value) for each sample was extracted using BRB-ArrayTools along with the molecular subtype assignment. EGFR expression was plotted as a

function of molecular subtype, and one-way ANOVA with Tukey's Multiple Comparisons post-hoc test was performed using GraphPad Prism version 5.00 for Windows (GraphPad Software, CA, USA, www.graphpad.com).

Immunohistochemical (IHC) analysis of EGFR expression in patient tumors

Approval was obtained from the Human Research Ethics Committee of the Royal Brisbane & Women's Hospital and The University of Queensland to use human breast tumor samples for research. Tissue microarrays (TMAs) were enriched for high-grade invasive ductal carcinomas for which ER, PR and HER2 IHC data was also available. Standard IHC was performed on TMA sections to evaluate EGFR protein expression in breast tumors. Briefly, after antigen retrieval (chymotrypsin for 10 min at 105°C), IHC was done using the anti-EGFR primary antibody (clone 31G7, Invitrogen^{TM}; 1:100 dilution, 1 h incubation at RT) and the MACH 2™ Polymer Detection system according to the manufacturer's protocol (Biocare Medical, CA, USA). Staining was visualized with 3,3′-Diaminobenzidine (DAB) and a hematoxylin counterstain. The staining was assessed semi-quantitatively by recording the intensity and percentage of cells stained.

DNA-damage, clonogenic survival, apoptosis and cell death assays in vitro

Sub-confluent cultures of MDA-MB-231 cells were treated with doxorubicin at 5 nM, docetaxel at 1 nM and PARPi at 350 nM. For ^{177}Lu-anti-EGFR RIT, the activity required to achieve 4 Gy over 72 h was 19.7 μCi calculated based on the dose rate constant of ^{177}Lu being 0.283 g·rad/μCi·h: ($0.283\ \frac{\text{g x Rad}}{\mu\text{Ci x h}}$ x 19.7 μCi x 72 h ÷ 1 g = 401.4 Rad ÷ 100 = 4.01 Gy, assuming the weight of 1 mL of culture media is 1 g. The concentration of the EGFR mAb in culture media to achieve 4 Gy ranged between 6.6 to 9.9 μg/mL. Thus, 10 μg/mL of unlabeled anti-EGFR mAb was used as a negative control for RIT in vitro. For in vitro treatments without RIT, chemotherapy, PARPi or chemotherapy and PARPi were added to cell cultures for 6 h before removal and replenishment with drug-free media containing 10 μg/mL of unlabeled anti-EGFR mAb. For treatments with RIT, cell cultures were treated with chemotherapy, PARPi or chemotherapy 6 h then replenished with drug-free media containing 19.7 μCi of ^{177}Lu-anti-EGFR mAb. Six hours after treatment with unlabeled or labeled anti-EGFR mAb, cells were replenished with drug-free media.

To assess double-strand DNA breaks, cells were treated as described above in chamber slides then collected at specified time points for fixation and permeabilization with ice-cold 100% methanol. After blocking with 1% bovine serum albumin solution in PBS, cells were incubated overnight at 4°C with 0.4 μg/mL solution of anti-γH2AX biotinylated mAb (Clone JBW301, Millipore, MA, USA). Cells were washed and incubated with 1 μg/mL of streptavidin-Alexa$_{488}$ (Invitrogen^{TM}) for 30 min at room temperature. Cells were washed extensively then slides were mounted using ProLong® Gold antifade reagent with DAPI (Invitrogen^{TM}) as per manufacturer instructions. Images were acquired using Deltavision PersonalDV microscope (Applied Precision Inc., GE Healthcare, Buckinghamshire, UK). For flow cytometric analysis of apoptosis (Annexin V and 7-AAD staining) and cell cycle, cells were collected at the specified time points and stained for flow cytometry as described earlier. Clonogenic survival was measured using standard assay. For cellular senescence, cytochemical detection of β-galactosidase activity was carried out as described elsewhere (*5*).

Supplemental Results

Preliminary safety and efficacy studies for the combination of chemotherapy, PARPi and anti-EGFR RIT

Combination of docetaxel at 2 mg/kg and doxorubicin at 10 mg/kg was synergistic compared to single agents alone at these doses. In fact, this combination reduced tumor growth rate to a level comparable to treatment with 8 mg/kg of docetaxel alone but without any associated weight loss (Supplemental Figures 5A and 5B). Similar synergy was observed when combining 4 mg/kg docetaxel and 20 mg/kg doxorubicin. Next, we investigated these two regimens in combination with PARPi. PARPi (PF-01367338, Pfizer) administered at 1 mg/kg daily for 5 days was well tolerated and potentiated both half-dose (2 mg/kg docetaxel and 10 mg/kg doxorubicin) and full-dose (4 mg/kg docetaxel and 20 mg/kg doxorubicin) chemotherapy to comparable levels (Supplemental Figures 5A and 5B). The addition of ^{177}Lu-anti-EGFR RIT (using the mouse monoclonal antibody 225, the precursor to cetuximab) at either 300 or 450 MBq/kg (6 or 9 MBq per 20-g mouse, respectively) to full-dose chemotherapy and PARPi led to reversible but significant weight loss (15%). Nevertheless, the combination of half-dose chemotherapy and PARPi with ^{177}Lu-anti-EGFR RIT at 300 MBq/kg and 450 MBq/kg was efficacious and well tolerated (Supplemental Figures 5C and 5D). Based on these studies, we determined that 2 mg/kg docetaxel and 10 mg/kg doxorubicin chemotherapy and 300 MBq/kg ^{177}Lu-anti-EGFR RIT were suitable to investigate with PARPi.

Triple-agent combination causes significant DNA damage and loss of clonogenic survival

To determine the effect of the combination therapy on the induction of DNA damage and its repair, we treated exponentially growing MDA-MB-231 cell cultures *in vitro* then removed the cytotoxic drugs before replenishing the cells with drug-free media. The triple-agent combination caused significantly more DNA double-strand breaks (DSBs) as detected by antibody against phosphorylated H2AX (γ-H2AX) compared to other treatments (Supplemental Figures 7A and 7B). This combination also showed a delay in the repair of these breaks (Supplemental Figure 7C) with DSBs persisting at 12 hours after removal of the triple-agent combination. In concordance elevated DNA damage, MDA-MB-231 cells treated with the triple-agent combination showed a significant increase in proportions of early apoptotic cells (Annexin V+/7-AAD-) and the subG1 population (DNA fragmentation, <G1) and a significant loss of clonogenic survival (Supplemental Figures 7D and 7E). We did not observe any increase in senescence (β-galactosidase staining) with any of the treatments in comparison to untreated cells (data not shown).

Supplemental Figures

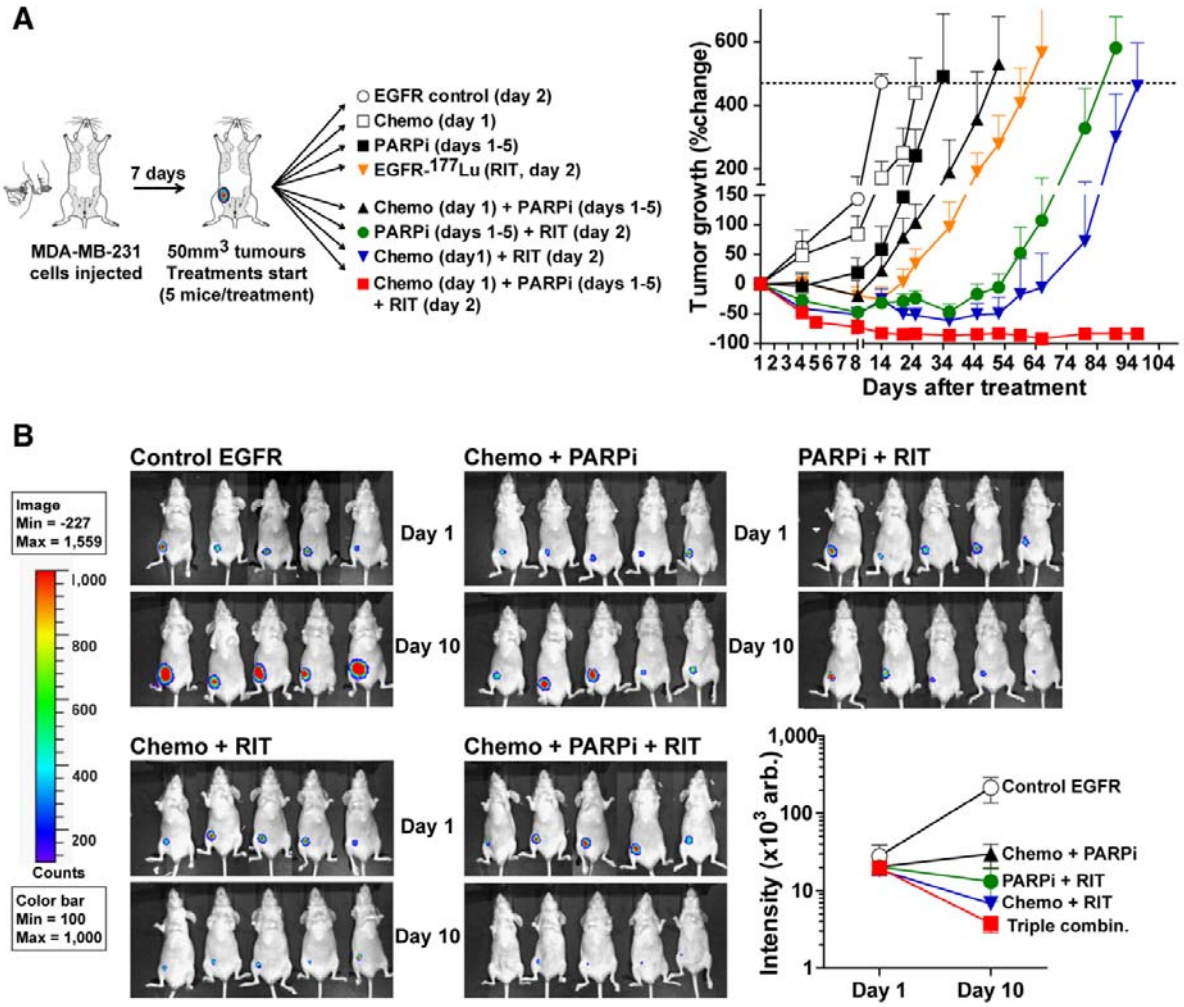

Supplemental Figure 1: Eradication of MDA-MB-231 mammary fat pad xenografts using the combination of EGFR directed RIT with chemotherapy and PARPi. Female nude BALB/c mice bearing MDA-MB-231 mammary fat pad tumors (5 mice per group) were untreated (vehicle control, data not shown), treated with unlabeled anti-EGFR mAb (EGFR control), doxorubicin (10 mg/kg) and docetaxel (2 mg/kg) chemotherapy (chemo), PARP inhibitor at 2 mg/kg daily for 5 days (PARPi) or 300 MBq/kg ^{177}Lu-anti-EGFR mAb (RIT). Treatment schedules are depicted in the diagram in panel A. Any treatment without RIT included unlabeled anti-EGFR mAb as a control. Mouse weights (data not shown, no significant weight loss observed) and tumor volumes were monitored. (**A**) Tumor growth curves. Data shown are the average percentage change (± SEM, n = 5 mice/treatment) in tumor volume (**B**) Bioluminescence imaging of mice and mean luminescence intensities (±SEM, n = 5/group) on day 1 and on day 10 after treatment.

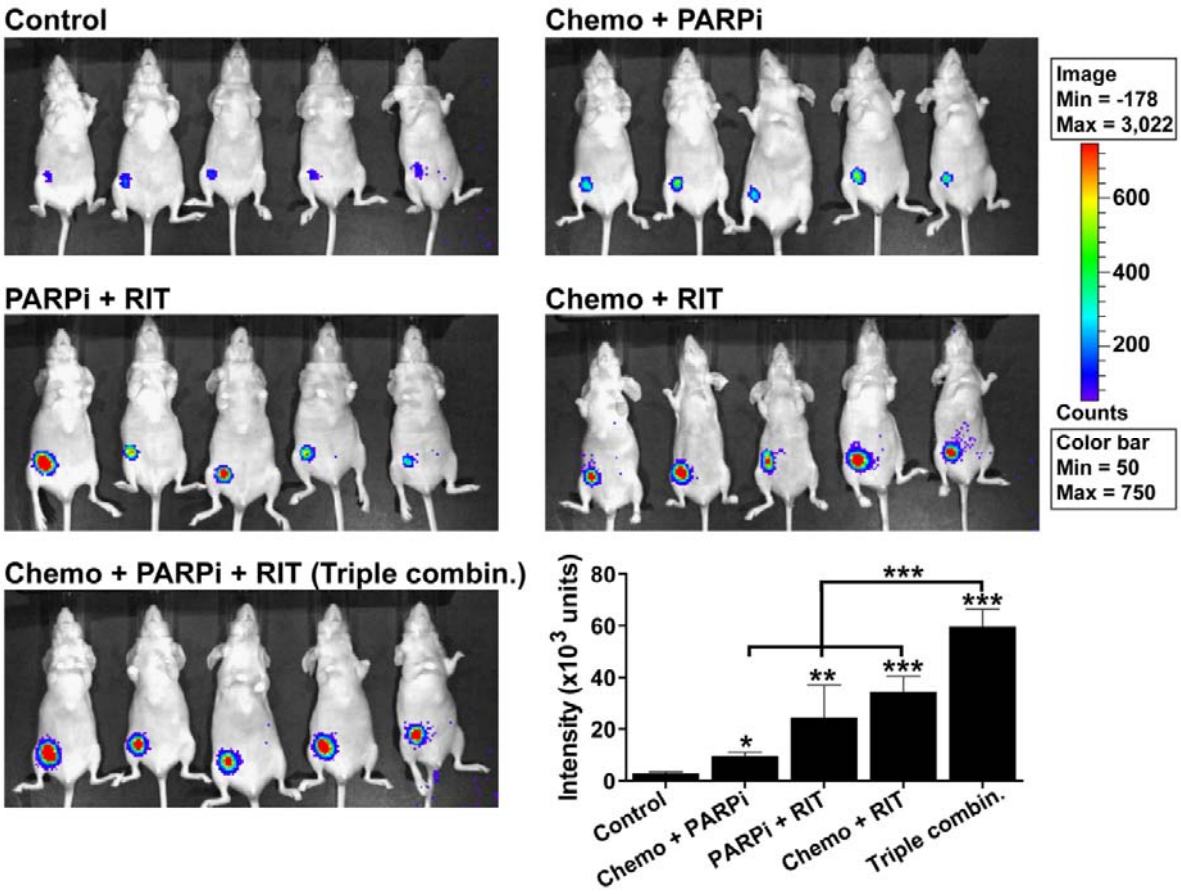

Supplemental Figure 2: *In vivo* bioluminescent imaging (BLI) of caspase-3/7 activation after treatment. Female nude BALB/c mice bearing Luciferase-expressing mammary fat pad xenografts of MDA-MB-231 were left untreated or treated as indicated. Treatment doses, schedule and routes of administration were as described in Legend to Figure 1. Seven days after treatment (5 mice/group), mice were injected with VivoGlo™ Caspase 3/7 substrate (25 mg/kg) and imaged 10 min later. The mean luminescence intensities (±SEM, n = 5) for caspase-3 activation were summarized in the bar graph (* $p < 0.05$, ** $p < 0.01$, *** $p < 0.001$, one-way ANOVA with Tukey's multiple comparisons post test using GraphPad Prism).

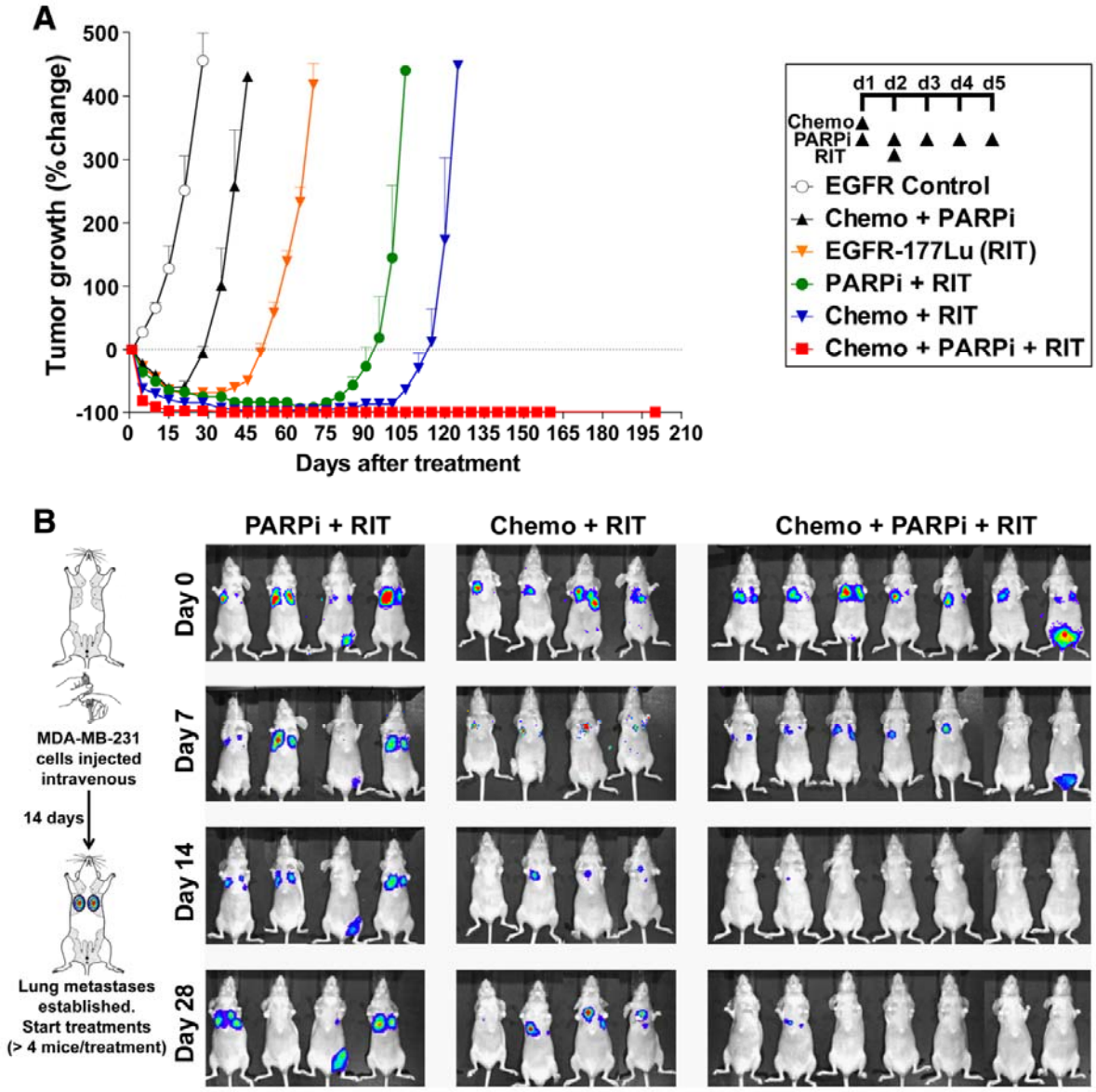

Supplemental Figure 3: Treatment of patient-derived orthotopic grafts and established MDA-MB-231 metastases using the triple combination therapy. (A) Mice bearing patient-derived HCI-002 grafts in the mammary fat pads were treated as described in Figure 1 (n = 10 per treatment group) and tumors were monitored for growth using caliper measurements. The triple agent combination stopped the recurrences observed in all the other treatment arms. **(B)** In a separate model, established metastases (14 days after intravenous injection of MDA-MB-231 cells) were visualized by bioluminescent imaging. Treatments were initiated immediately after imaging (day 0) and mice were imaged weekly thereafter. The combination of EGFR-directed RIT with PARPi or with chemotherapy showed a transient anti-tumor effect on lung metastases while the triple-agent combination eliminated these metastases with no recurrences observed up to 42 days after treatment.

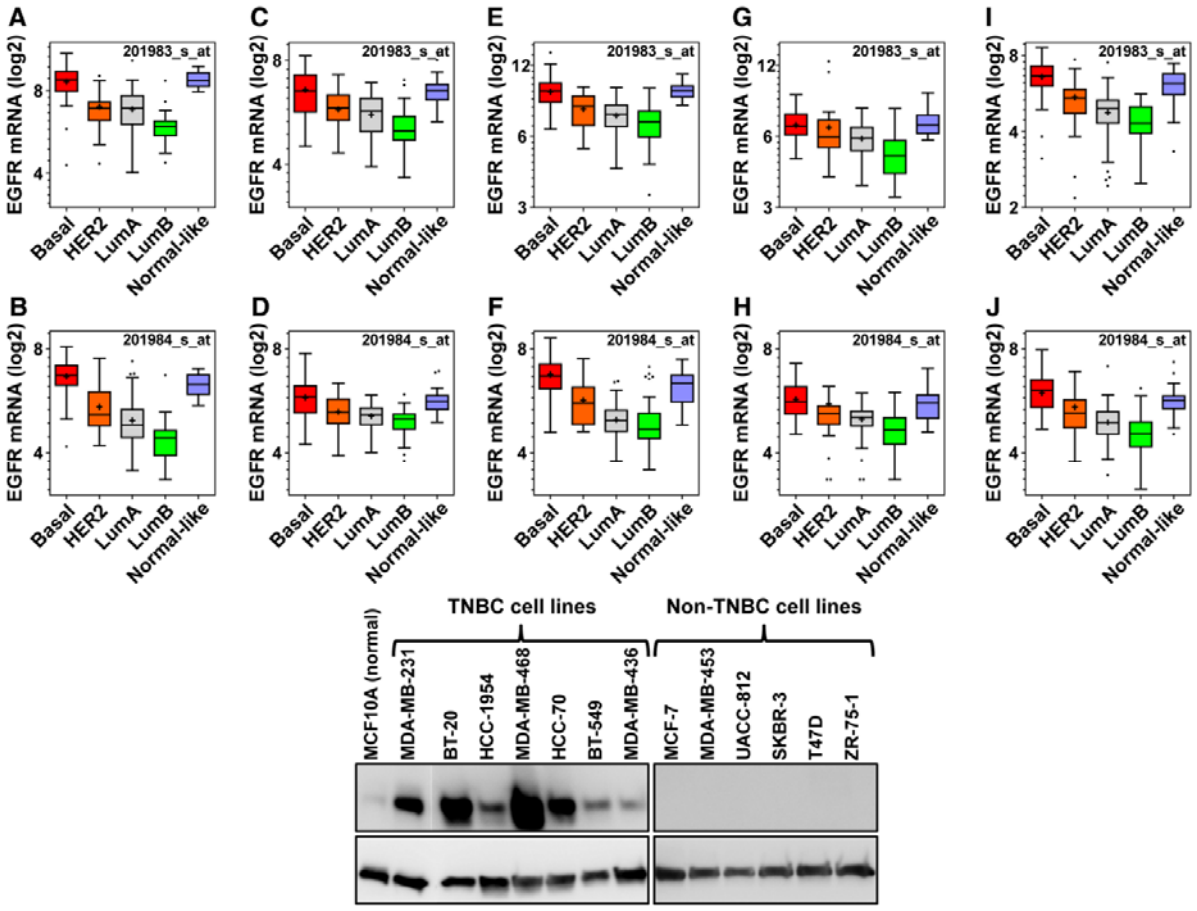

Supplemental Figure 4: EGFR mRNA expression in publicly available gene expression array studies is correlated with basal-like breast cancer. Data shown are from two *EGFR*-specific probes; 201983_s_at in upper panels (A, C, E, G and I) or 201984_s_at in lower panels (B, D, F, H and J). The five different datasets are shown in the five columns; **A&B**: Bos et al. (*6*) (GSE12276), **C&D**: Sabatier et al. (*7*) (GSE21653), **E&F**: Sotiriou et al. (*8*) (GSE2990), **G&H**: Miller et al. (*9*) (GSE3494) and **I&J**: Wang et al. (*10*) (GSE2034). EGFR mRNA is significantly higher in the basal-like molecular subtype (Basal) compared to HER2, Luminal A (LumA) and Luminal B (LumB) subtypes, but not compared to the normal-like subtype. Bottom panel shows immunoblot of breast cancer cell lines with anti-EGFR clone 225 mAb.

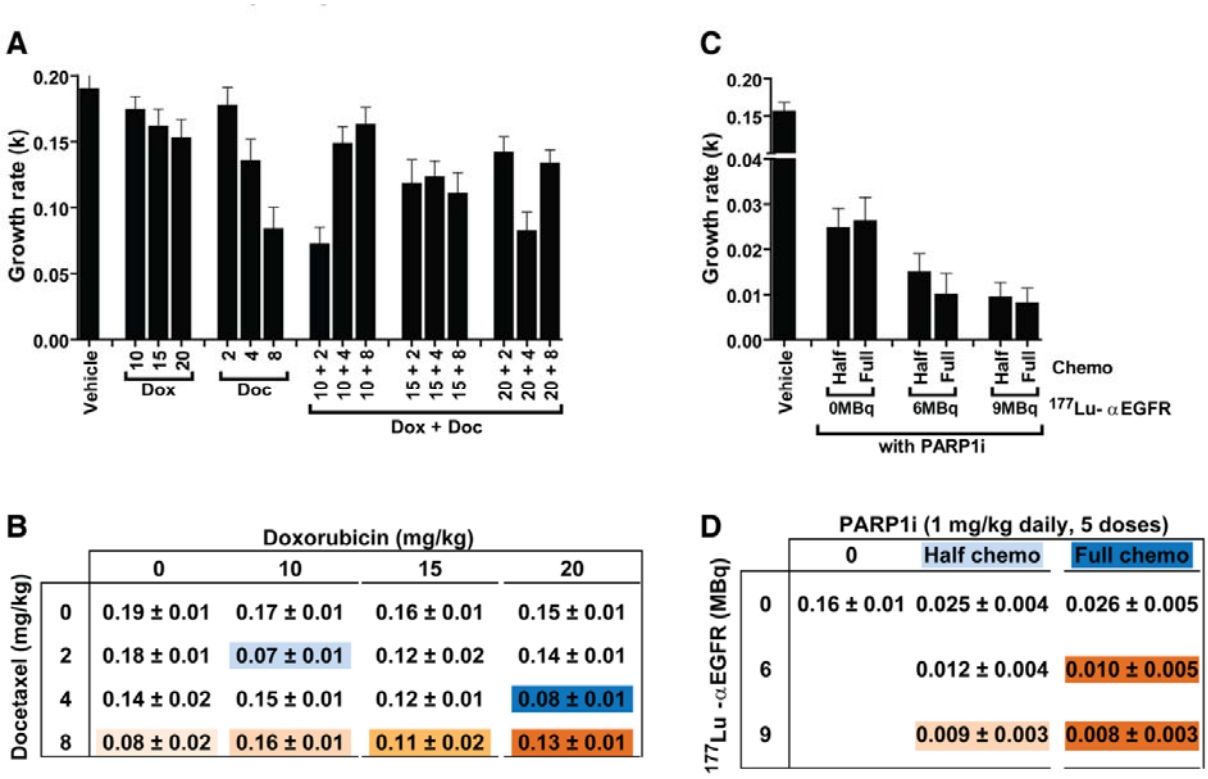

Supplemental Figure 5: Maximum tolerated studies to deduce safe and effective combination therapy using chemotherapy, PARPi and anti-EGFR RIT. (A) Female nude BALB/c mice bearing MDA-MB-231 mammary fat pad tumors (5 mice per group) were untreated (vehicle control) or treated with 10, 15 or 20 mg/kg Doxorubicin alone (Dox); 2, 4 or 8 mg/kg of Docetaxel alone (Doc) or combined (Dox+Doc). Exponential growth curves were fitted by GraphPad Prism to produce the tumor growth rate (k). (**B**) Summary of the 'k' (+SEM) data in A where toxic treatments are marked by shades of orange to denote increasing toxicity. Two safe and synergistic combined doses of Doxorubicin and Docetaxel are marked in blue. (**C**) The two safe combined chemotherapy doses were investigated in a second study in combination with PARPi (AG014699, Pfizer; 1 mg/kg daily, 5 doses) alone or in combination with 6 or 9 MBq per 20 g mouse dose of ^{177}Lu-anti-EGFR mAb (^{177}Lu-αEGFR). (**D**) Summary of the growth rate (k) of tumors with orange shading marking toxic treatments. PARPi was well tolerated and potentiated both half-dose (2 mg/kg docetaxel and 10 mg/kg doxorubicin) and full-dose (4 mg/kg docetaxel and 20 mg/kg doxorubicin) chemotherapy to comparable levels.

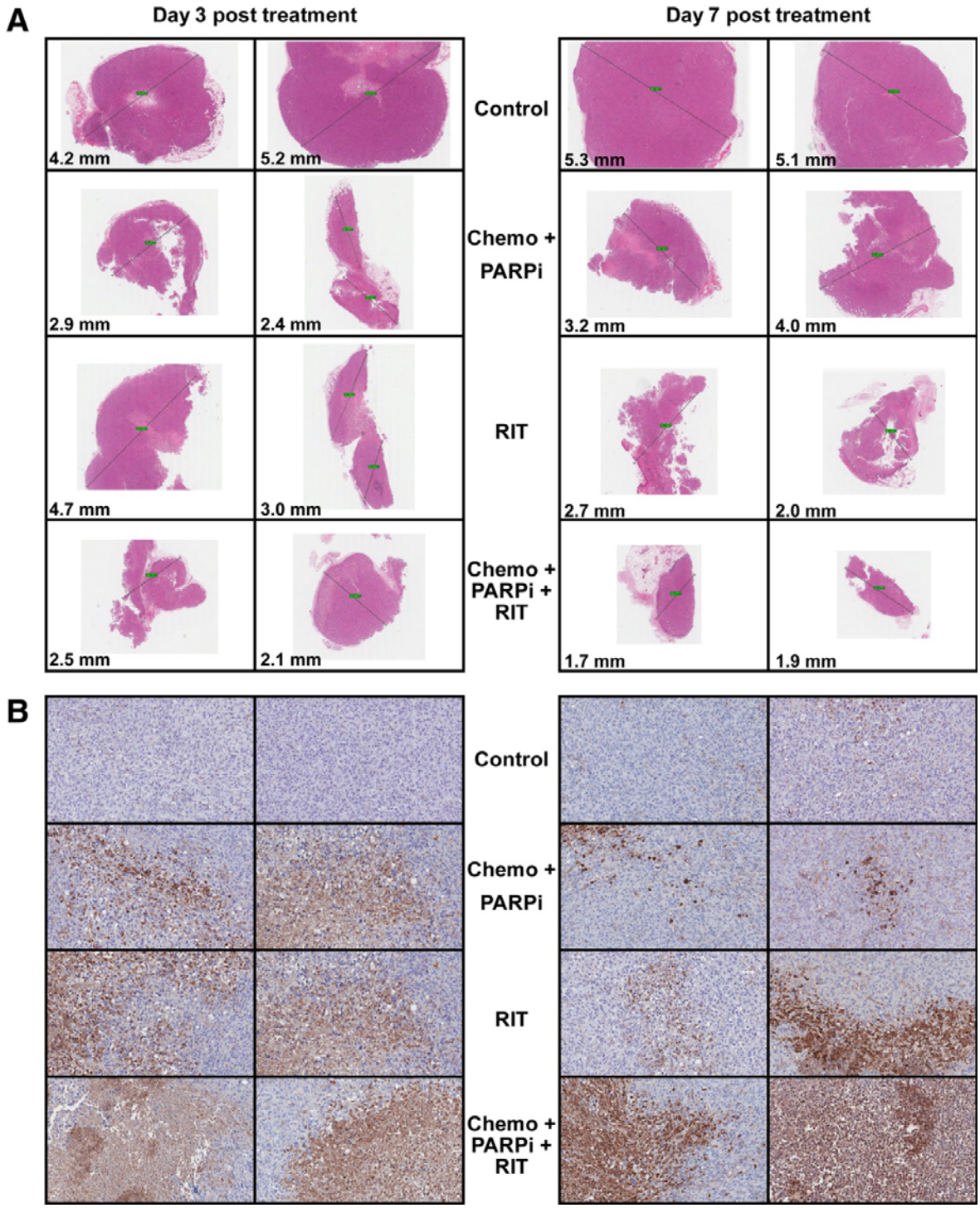

Supplemental Figure 6: Representative H&E and cleaved PARP1 IHC in MDA-MB-231 mammary fat pad xenografts collected at 3 and 7 days post treatment. Images are shown for two different mice at each treatment condition. All images shown are obtained under identical magnification; (**A**) 4X for H&E sections (tumor diameter is shown in mm as measured using Aperio ImageScope), (**B**) 20X for cleaved PARP-1 IHC. Images of ten random regions from each slide were analyzed using ImageJ (*11*) (V1.46d) with ImmunoRatio plug-in (*12*). Percentage of cells staining positive for cleaved PARP-1 was measured and data were summarized in Figure 3.

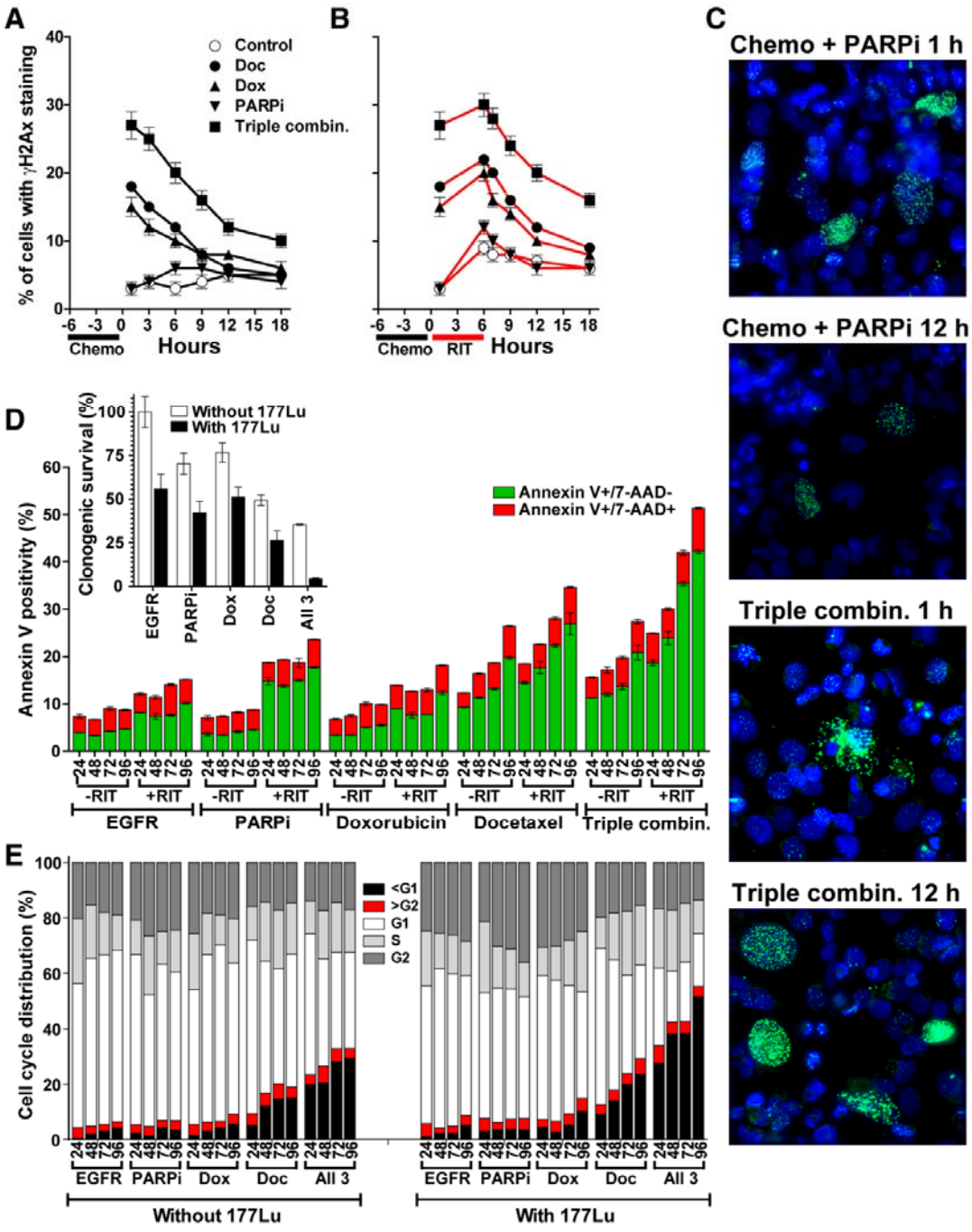

Supplemental Figure 7: DNA-damage, cell death, clonogenic survival and cell cycle after treatment of MDA-MB-231 cells with the combination of chemotherapy, PARPi and EGFR-directed RIT. Cultures of MDA-MB-231 cells were treated as described in Methods. (**A&B**) γH2AX foci formation and resolution as a measure of DNA double strand breaks and repair. Data shown are the mean (±SEM, n = 3) for cells treated with agents and (**A**) unlabeled anti-EGFR mAb or (**B**) ^{177}Lu-anti-EGFR mAb RIT. (**C**) Representative images of cells at 1 and 12 hours after treatment; γH2AX foci appear in green and nuclei appear in blue. (**D**) Annexin V and 7-AAD staining. Data shown are the mean ± SEM (n = 3). **Inset**: Clonogenic survival (mean ±SEM, n = 3) measured as the percentage of colonies forming at 10 days after treatment compared to control using standard clonogenic survival assay. (**E**) Cell cycle analysis by DNA content. Data shown are the mean (n = 3; SEM of the mean is not shown for clarity but did not exceed 1% for all data).

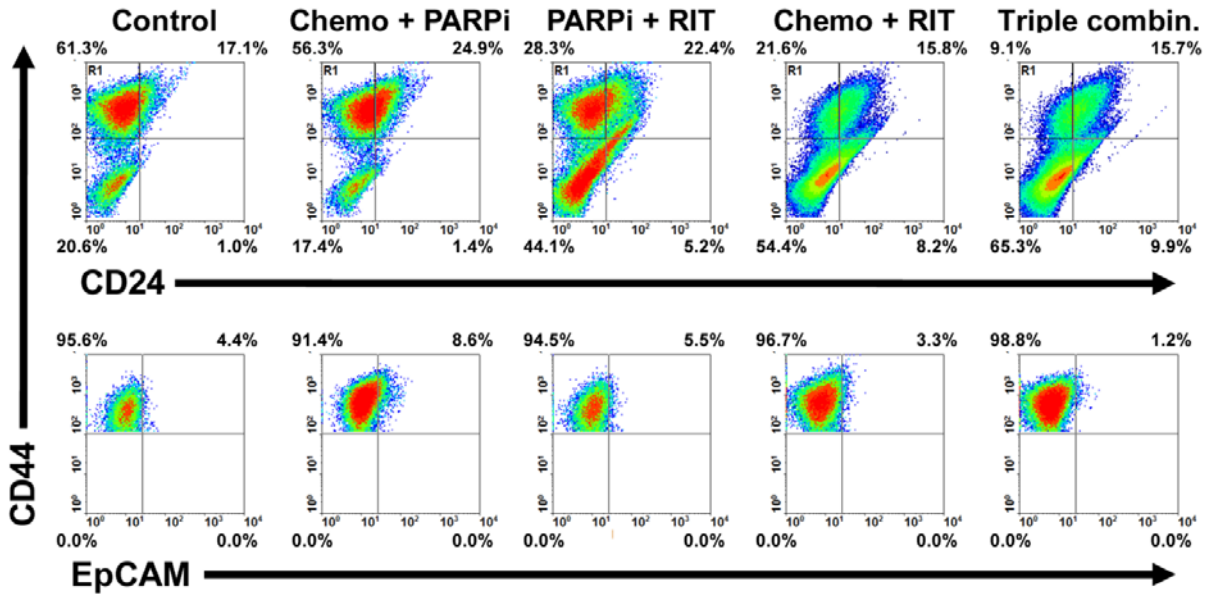

Supplemental Figure 8: Representative density plots of breast cancer stem cell marker staining of MDA-MB-231 tumor cell suspensions. Single cell suspensions from tumors isolated 16 days after treatment were stained with CD44, CD24 and EpCAM antibodies then analyzed by flow cytometry. Isotype-matched negative control antibodies were used to set quadrants as per the background staining. CD44 staining vs. CD24 staining in the upper panels was used to select for $CD44^{+}/CD24^{-}$ cells (R1) and these cells were analyzed for EpCAM staining in the lower panels.

Supplemental References

1. Al-Ejeh F, Darby JM, Thierry B, Brown MP. A simplified suite of methods to evaluate chelator conjugation of antibodies: effects on hydrodynamic radius and biodistribution. *Nucl Med Biol.* 2009;36:395-402.

2. DeRose YS, Wang G, Lin YC, et al. Tumor grafts derived from women with breast cancer authentically reflect tumor pathology, growth, metastasis and disease outcomes. *Nat Med.* 2011;17:1514-1520.

3. Zhao Y, Simon R. BRB-ArrayTools Data Archive for human cancer gene expression: a unique and efficient data sharing resource. *Cancer Inform.* 2008;6:9-15.

4. Hu Z, Fan C, Oh DS, et al. The molecular portraits of breast tumors are conserved across microarray platforms. *BMC Genomics.* 2006;7:96-107.

5. Debacq-Chainiaux F, Erusalimsky JD, Campisi J, Toussaint O. Protocols to detect senescence-associated beta-galactosidase (SA-betagal) activity, a biomarker of senescent cells in culture and in vivo. *Nat Protoc.* 2009;4:1798-1806.

6. Bos PD, Zhang XH, Nadal C, et al. Genes that mediate breast cancer metastasis to the brain. *Nature.* 2009;459:1005-1009.

7. Sabatier R, Finetti P, Cervera N, et al. A gene expression signature identifies two prognostic subgroups of basal breast cancer. *Breast Cancer Res Treat.* 2011;126:407-420.

8. Sotiriou C, Wirapati P, Loi S, et al. Gene expression profiling in breast cancer: understanding the molecular basis of histologic grade to improve prognosis. *Journal of the National Cancer Institute.* 2006;98:262-272.

9. Miller LD, Smeds J, George J, et al. An expression signature for p53 status in human breast cancer predicts mutation status, transcriptional effects, and patient survival. *Proc Natl Acad Sci U S A.* 2005;102:13550-13555.

10. Wang Y, Klijn JG, Zhang Y, et al. Gene-expression profiles to predict distant metastasis of lymph-node-negative primary breast cancer. *Lancet.* 2005;365:671-679.

11. Abramoff MD, Magalhaes PJ, Ram SJ. Image Processing with ImageJ. *Biophonotics International.* 2004;11:36-43

12. Tuominen VJ, Ruotoistenmaki S, Viitanen A, Jumppanen M, Isola J. ImmunoRatio: a publicly available web application for quantitative image analysis of estrogen receptor (ER), progesterone receptor (PR), and Ki-67. *Breast Cancer Res.* 2010;12:R56-R67.